Journal of Visualized Experiments

Real-Time Assessment of Spinal Cord Microperfusion in a Porcine Model of Ischemia/Reperfusion

--Manuscript Draft--

Article Type:	Invited Methods Article - JoVE Produced Video
Manuscript Number:	JoVE62047R1
Full Title:	Real-Time Assessment of Spinal Cord Microperfusion in a Porcine Model of Ischemia/Reperfusion
Corresponding Author:	Christoph R. Behem University Medical Center Hamburg-Eppendorf: Universitatsklinikum Hamburg-Eppendorf Hamburg, Hamburg GERMANY
Corresponding Author's Institution:	University Medical Center Hamburg-Eppendorf: Universitatsklinikum Hamburg-Eppendorf
Corresponding Author E-Mail:	c.behem@uke.de
Order of Authors:	Christoph R. Behem
	Till Friedheim
	Sabine Wipper
	Hans Pinnschmidt
	Michael Graessler
	Catharina Gaeth
	Hannes Holthusen
	Adina Rapp
	Timo Suntrop
	Josephina Haunschild
	Christian Etz
	Constantin Trepte
Additional Information:	
Question	**Response**
Please specify the section of the submitted manuscript.	Medicine
Please indicate whether this article will be Standard Access or Open Access.	Standard Access (US$2,400)
Please indicate the **city, state/province, and country** where this article will be **filmed**. Please do not use abbreviations.	Hamburg, Hamburg, Germany
Please confirm that you have read and agree to the terms and conditions of the author license agreement that applies below:	I agree to the Author License Agreement
Please provide any comments to the journal here.	

TITLE:

Real-Time Assessment of Spinal Cord Microperfusion in a Porcine Model of Ischemia/Reperfusion

AUTHORS AND AFFILIATIONS:

Christoph R. Behem[1], Till Friedheim[1], Sabine H. Wipper[2], Hans O. Pinnschmidt[3], Michael F. Graessler[1], Catharina Gaeth[4], Hannes Holthusen[1], Adina Rapp[5], Timo Suntrop[1], Josephina Haunschild[6], Christian D. Etz[6], Constantin J. C. Trepte[1]

[1]Department of Anesthesiology, Center of Anesthesiology and Intensive Care Medicine, University Medical Center Hamburg-Eppendorf, Hamburg, Germany
[2]University Department for Vascular Surgery, Department of Operative Medicine, Medical University of Innsbruck, Austria
[3]Department of Medical Biometry and Epidemiology, University Medical Center Hamburg-Eppendorf, Hamburg, Germany
[4]Department of Vascular Medicine, University Heart and Vascular Center Hamburg (UHZ), Hamburg, Germany
[5]Department of Cardiology, Rostock University Medical Center, Rostock, Germany
[6]University Department for Cardiac Surgery, Heart Center Leipzig, Leipzig, Germany.

Corresponding Author:
Christoph R. Behem
c.behem@uke.de

Email Addresses of Co-authors:
t.friedheim@uke.de
sabine.wipper@i-med.ac.at
h.pinnschmidt@uke.de
m.graessler@uke.de
catharina.gaeth@web.de
hannes.holthusen@gmx.de
Adina.rapp@med.uni-rostock.de
6699344@stud.uke.uni-hamburg.de
Josephina.Haunschild@medizin.uni-leipzig.de
Christian.Etz@medizin.uni-leipzig.de
c.trepte@uke.de

KEYWORDS:

Spinal cord injury, spinal cord ischemia, spinal cord perfusion, hemodynamic therapy, microcirculation, cerebrospinal fluid pressure, Laser-Doppler

SUMMARY:

Spinal cord microcirculation plays a pivotal role in spinal cord injury. Most methods do not allow real-time assessment of spinal cord microcirculation, which is essential for the development of microcirculation-targeted therapies. Here, we propose a protocol using Laser-Doppler-Flow Needle probes in a large animal model of ischemia/reperfusion.

ABSTRACT:
Spinal cord injury is a devastating complication of aortic repair. Despite developments for the prevention and treatment of spinal cord injury, its incidence is still considerably high and therefore, influences patient outcome. Microcirculation plays a key role in tissue perfusion and oxygen supply and is often dissociated from macrohemodynamics. Thus, direct evaluation of spinal cord microcirculation is essential for the development of microcirculation-targeted therapies and the evaluation of existing approaches in regard to spinal cord microcirculation. However, most of the methods do not provide real-time assessment of spinal cord microcirculation. The aim of this study is to describe a standardized protocol for real-time spinal cord microcirculatory evaluation using laser-Doppler needle probes directly inserted in the spinal cord. We used a porcine model of ischemia/reperfusion to induce deterioration of the spinal cord microcirculation. In addition, a fluorescent microsphere injection technique was used. Initially, animals were anesthetized and mechanically ventilated. Thereafter, laser-Doppler needle probe insertion was performed, followed by the placement of cerebrospinal fluid drainage. A median sternotomy was performed for exposure of the descending aorta to perform aortic cross-clamping. Ischemia/reperfusion was induced by supra-celiac aortic cross-clamping for a total of 48 min, followed by reperfusion and hemodynamic stabilization. Laser-Doppler Flux was performed in parallel with macrohemodynamic evaluation. In addition, automated cerebrospinal fluid drainage was used to maintain a stable cerebrospinal pressure. After completion of the protocol, animals were sacrificed, and the spinal cord was harvested for histopathological and microsphere analysis. The protocol reveals the feasibility of spinal cord microperfusion measurements using laser-Doppler probes and shows a marked decrease during ischemia as well as recovery after reperfusion. Results showed comparable behavior to fluorescent microsphere evaluation. In conclusion, this new protocol might provide a useful large animal model for future studies using real-time spinal cord microperfusion assessment in ischemia/reperfusion conditions.

INTRODUCTION:
Spinal cord injury induced by ischemia/reperfusion (SCI) is one of the most devastating complications of aortic repair associated with reduced outcome[1-4]. Current prevention and treatment options for SCI include the optimization of macrohemodynamic parameters as well as the normalization of cerebrospinal fluid pressure (CSP) to improve spinal cord perfusion pressure[2,5-9]. Despite the implementation of these maneuvers, incidence of SCI still ranges between 2% and 31% depending on the complexity of aortic repair[10-12].

Recently, microcirculation has gained increased attention[13,14]. Microcirculation is the area of cellular oxygen uptake and metabolic exchange and therefore, plays a critical role in organ function and cellular integrity[13]. Impaired microcirculatory blood flow is a major determinant of tissue ischemia associated with increased mortality[15-19]. Impairment of spinal cord microcirculation is associated with reduced neurological function and outcome[20-23]. Therefore, optimization of microperfusion for the treatment of SCI is a most promising approach. Persistence of microcirculatory disturbances, despite macrocirculatory optimization, has been described[24-27]. This loss of hemodynamic coherence occurs frequently in various conditions including ischemia/reperfusion, emphasizing the need for direct microcirculatory evaluation and microcirculation-targeted therapies[24,25,28].

So far, only few studies have used laser-Doppler probes for real-time assessment of spinal cord microcirculatory behavior[20,29]. Existing studies have often used microsphere injection techniques, which are limited by intermittent use and post-mortem analysis[30,31]. The number of different measurements using microsphere injection technique is limited by the availability of microspheres with different wavelengths. Moreover, in contrast to Laser-Doppler techniques, real-time assessment of microperfusion is not possible, as post-mortem tissue processing and analysis is needed for this method. Here, we present an experimental protocol for the real-time assessment of spinal cord microcirculation in a porcine large animal model of ischemia/reperfusion.

This study was part of a large animal project combining a randomized study comparing the influence of crystalloids vs. colloids on microcirculation in ischemia/reperfusion as well as an explorative randomized study on the effects of fluids vs. vasopressors on spinal cord microperfusion. Flow probe 2-point calibration as well as pressure-tip catheter calibration has been previously described[32]. In addition to the reported protocol, fluorescent microspheres were used for the measurement of spinal cord microperfusion, as previously described, using 12 samples of spinal cord tissue for each animal, with samples 1–6 representing the upper spinal cord and 7–12 representing the lower spinal cord[33,34]. Microsphere injection was performed for each measurement step after the completion of Laser-Doppler recordings and macrohemodynamic evaluation. Histopathological evaluation was performed using the Kleinman-Score as previously described[35].

PROTOCOL:

The study was approved by the Governmental Commission on the Care and Use of Animals of the City of Hamburg (Reference-No. 60/17). The animals received care in compliance with the 'Guide for the Care and Use of Laboratory Animals' (NIH publication No. 86–23, revised 2011) as well as FELASA recommendations and experiments were carried out according to the ARRIVE guidelines[22,23]. This study was an acute trial, and all animals were euthanized at the end of protocol.

NOTE: The study was performed in six three-month-old male and female pigs (German Landrace) weighing approximately 40 kg. Animals were brought to the animal care facilities at least 7 days prior to the experiments and were housed in accordance to animal welfare recommendations. Animals were provided food and water ad libitum, and their health status was regularly assessed by the responsible veterinarian. A fasting time of 12 h was maintained prior to the experiments. The entire experimental procedure and handling of the animals was supervised by the responsible veterinarian.

1. Anesthesia induction and maintenance of anesthesia

1.1. For anesthesia induction and maintenance of anesthesia, premedicate the animals and deeply sedate them using an intramuscular injection followed by intravenous injections, if necessary, to perform endotracheal intubation. Thereafter, induce and maintain anesthesia by using a combination of a volatile anesthesia agent with a continuous opioid application complemented with an additional opioid bolus injection.

1.2. Perform intramuscular injections of ketamine 20 $mg \cdot kg^{-1}$, azaperone 4 $mg \cdot kg^{-1}$, and midazolam 0.1 $mg \cdot kg^{-1}$ for premedication and sedation.

1.3. Place a venous catheter in an ear vein, secure proper fixation, and assess functionality by fast application of 10 mL of saline.

1.4. Place the animal in a supine position on a warming blanket to prevent heat loss.

1.5. Establish basic monitoring with electrocardiography (ECG) and pulse oximetry to monitor the cardio-pulmonary state of the animals, and connect it to the basic monitoring hardware.

1.6. Administer 15 $L \cdot min^{-1}$ of oxygen via a pig-shaped mask for preoxygenation.

1.7. Inject intravenous boli of 0.1 $mg \cdot kg^{-1}$ of 1% propofol, if necessary, and perform endotracheal intubation.

1.8. Secure correct placement with end tidal capnography and auscultation, administer 0.1 mg of pancuronium, and ensure proper fixation of the endotracheal tube.

1.9. Establish volume-controlled ventilation using tidal volumes of 10 $mL \cdot kg^{-1}$ $bodyweight^{-1}$, a positive end-expiratory pressure of 10 cmH_2O, and a fraction of inspired oxygen (FiO_2) of 0.3 using the anesthesia machine. Adjust the ventilator frequency to maintain an end-expiratory carbon dioxide tension ($etCO_2$) of 35–45 mmHg.

1.10. Introduce a gastric tube, perform suction of gastric fluids, properly fix the tube, and connect it to a collection bag. Carefully close the animal's eyes to prevent dryness of eyes during anesthesia.

1.11. Maintain anesthesia by continuous infusion of fentanyl (10 $\mu g \cdot kg^{-1} \cdot h^{-1}$) and sevoflurane (3.0% expired concentration, delivered by the vapor). Ensure adequate level of anesthesia by careful observation of vital signs and ventilation parameters as well as by absence of any movements during the entire protocol, paying special attention to the phases of surgical stimulus. Give additional bolus doses of fentanyl (50 µg) if there is any indication of pain or distress.

NOTE: Ensure the presence of researchers who are experienced in animal anesthesia during the entire procedure, and use supervision by an experienced veterinarian to secure proper anesthesia.

1.12. Administer a baseline infusion rate of 10 $mL \cdot kg^{-1} \cdot h^{-1}$ balanced crystalloids to compensate for fluid losses during anesthesia, surgical preparation, and execution of the experimental protocol. Use a fluid warmer to prevent heat loss.

1.13. Gently clean the pig's skin using soap water. Use a skin disinfection solution containing povidone-iodine to decrease skin contamination. Use sterile gloves for surgical preparations. Apply 300 mg of clindamycin as antimicrobial prophylaxis, and repeat the dosage after 6 h.

2. Probe placement

2.1. Place the animal in the right lateral position, and flex the animal's back to widen the space between the vertebrae.

2.2. Surgically expose the paravertebral area for the preparation of spinous processes and vertebral arches (**Figure 1A**).

2.3. Place a vascular 14 G peripheral vein catheter paramedian into the spinal cord at the level of thoracic vertebra (Th) 13/14 or lumbar vertebra (L) 1/2 between two vertebral arches (**Figure 1B**).

2.4. Remove the needle, insert the laser/Doppler needle probe over the vein catheter (**Figure 1C**), and test the signal quality by connection to the designated hard- and software. Ensure that there is a stable signal with moderate pulsatility.

2.5. Carefully fix the probe with sutures (**Figure 1D**) and use padding to prevent dislocation or kinking of the probe.

2.6. For percutaneous placement of cerebrospinal fluid drainage for measuring and controlling cerebrospinal pressure, identify the level of L 4/5 or L 5/6, puncture the skin and the subcutaneous space with the introducer needle, and remove the inlay needle.

2.7. Place a saline-filled syringe on the needle, and carefully introduce the needle with constant pressure on the fluid-filled syringe.

2.8. Once a loss of resistance is felt as evidence for epidural position, re-introduce the inlay needle, and introduce the needle 2–3 mm further to puncture the dura mater and remove the inlay needle.

2.9. Verify intrathecal position by fast dripping of clear liquor. Introduce the drainage up to 20 cm depth, attach the Luer-lock adapter, and verify the position by careful aspiration of liquor.

2.10. Carefully fix the drainage with sutures, and connect it to the cerebrospinal fluid drainage system.

2.11. Expose the skull behind the left ear, and carefully perform a drill hole trepanation of the skin using a 6 mm drill attachment.

2.12. Introduce a second laser doppler probe directly into the brain. Carefully fix the probe with sutures, and test the signal quality by connection to designated hard- and software. Again, make sure that there is a stable signal with moderate pulsatility.

2.13. Disconnect all probes, carefully place the animal in a supine position, ensuring unaffected probe position. Ensure that at least 4–5 researchers perform this maneuver.

2.14. Reconnect the probes, and re-check signal quality.

2.15. Connect the output channels of the laser-Doppler hardware to the amplifier and synchronic acquisition hardware and software to additionally record laser/Doppler Flux simultaneously with macrohemodynamic signals.

2.16. Calibrate Flux as per unit (PU) with 2-point calibration.

2.16.1. Press **Enter** to open the menu and select the **analogue output setting**.

2.16.2. Use the displayed conversion factor (**5.0 V = 1000 PU**) to calibrate Flux with 2-point calibration for use with the synchronic acquisition software.

2.16.3. Select **Return** to return to the previous menu, and select **Measurement** to continue with measurement.

2.16.4. Open the **synchronic acquisition** software. Select **zero all inputs** from the **Setup** menu. Connect all inputs with the used devices and probes.

2.16.5. Perform 2-point calibration for Flux by clicking on the dropdown menu of the **Flux channel**. Select **2-point calibration**. Set **units-conversion** to **on** and select **BPU** as units. For **point 1**, set **0 V** to **0 BPU**. For **point 2**, set **5.0 V** to **1000 BPU**. Select **set units** for **all and new data**. Press **OK** to close the menu.

2.17. Start continuous cerebrospinal fluid drainage with a target pressure of 10 mmHg and drainage volume of 20 $mL \cdot h^{-1}$.

3. Catheter placement

3.1. Expose both femoral arteries.

3.2. Ligate the distal part of the right femoral artery, temporarily occlude the proximal lumen of the artery using a vessel loop, perform a 2 mm cut of the vessel using a Potts' scissor, and introduce the guide wire.

3.3. Introduce the guide wire further, ensuring resistance-free insertion and avoiding any kinking of the wire; introduce the catheter over the wire.

3.4. Fix the catheter with sutures.

3.5. Ensure correct position by aspiration of arterial blood verified with blood gas analysis and arterial signal measurement after proper connection to the blood pressure and trans-cardiopulmonary monitoring hard- and software.

3.6. Place a 5 mm flow-probe on the left femoral artery, and test the signal quality by connection to the flowmeter.

3.7. Close both groins with sutures.

3.8. Expose the right carotid artery as well as the right internal jugular vein for placement of 8 Fr. introducer sheaths.

3.9. For catheter placement, proceed in the same manner as described in 3.2–3.4.

3.10. Connect the side-lumen of the carotid artery introducer sheath to the basic pressure monitoring and pulmonary thermodilution hardware for arterial pressure measurement.

3.11. Introduce a pressure-tip catheter into the ascending aorta, and verify the position by connection to the amplifier and synchronic acquisition hard- and software.

3.12. Place a Swan-Ganz pulmonary artery catheter via the venous sheath in the pulmonary artery by inflating the balloon with air at 20 cm depth and gently inserting it until a wedge pressure is seen in the hemodynamic curve. Deflate the balloon and pull the catheter back 2 cm. Ensure satisfying signal quality of pulmonary artery pressure. Connect the thermistors to basic pressure monitoring and pulmonary thermodilution hardware.

3.13. Use sonographic guidance for percutaneous placement of a 12 Fr. 5-Lumen central venous catheter for drug administration and central venous pressure measurement into the external right jugular vein. Use the 6 step-approach for sonographic placement[36].

3.14. Connect the distal lumen of the catheter to the blood pressure and trans-cardiopulmonary monitoring hard- and software. Switch all drugs and infusions to the central venous catheter. Use different lumen for analgesics, fluids, and catecholamines, and spare the large lumen for administration of colloids during volume-loading steps.

4. Surgical preparation

4.1. Perform a mini-laparotomy, mobilize the bladder, insert a foley catheter for urine drainage, inflate the balloon with saline, and fix the catheter with pouch sutures.

4.2. Connect the catheter to a urine collection bag displaying the urine amount in mL.

4.3. Increase the FiO_2 to 1.0, and re-administer 0.1 $mg \cdot kg^{-1}$ pancuronium intravenously.

4.4. Perform a median sternotomy by using electrocautery for prepping down to the sternum. Gently dissect the sternum from the surrounding tissue. Perform retrosternal placement of a compress to prevent injuries.

4.5. Stop ventilation and divide the bone with an oscillating saw. Continue ventilation and reduce FiO_2 to 0.3. Use electrocautery to reduce bleeding, and seal the sternum with bone wax.

4.6. Carefully mobilize the apex of the left lung, and divide the left lateral part of the diaphragm to facilitate surgical exposure.

4.7. Expose the descending aorta proximal to the celiac trunk by gentle retraction of the left lung, ensuring undisturbed ventilation and avoiding trauma to the left lung (**Figure 2A**) and divide the surrounding tissue (**Figure 2B**). Administer 7 mL·kg^{-1} hydroxyethyl starch colloid if hemodynamic stabilization is needed.

4.8. Place an overhold around the descending aorta to ensure proper exposure (**Figure 2C**).

4.9. Attach a flow probe around the descending thoracic aorta (**Figure 2D**). Ensure proper signal quality by connection to the flow module and synchronic acquisition hard- and software. Use contact gel to improve signal quality if needed.

4.10. Attach a vessel loop around the descending aorta, distal to the flow probe to mark the area of aortic cross clamping.

5. Assessment and data acquisition

5.1. Zero all catheters and level catheters using fluid-filled lines placed at the right atrial level.

5.2. Place needle ECG electrodes and connect them to the synchronic acquisition hard- and software.

5.3. Assessment of trans-cardiopulmonary thermodilution as well as aortic flow and pressure measurements have been previously described [32].

5.4. For cardiac output measurement using pulmonary artery thermodilution, perform 3 injections with 10 mL of cold saline, and note the mean value displayed by basic monitoring hardware.

5.5. Start the laser-Doppler software by simply pressing **Start**, and set a mark for each measurement step by carefully labeling the steps as **M0** to **M5**.

6. Experimental protocol

6.1. Perform baseline measurements (M0).

6.2. Perform hemodynamic optimization using volume-loading steps of 7 mL·kg^{-1} hydroxyethyl starch colloid. Perform each volume-loading step over 5 min using pressurized infusions. After completion of each volume-loading step, allow 5 min for equilibration. Commence volume loading until the increase in cardiac output is <15%.

6.3. Repeat measurements (M1) after completion of hemodynamic optimization.

6.4. Induce ischemia/reperfusion for a total of 48 min of supra-celiac aortic cross-clamping by placing an aortic clamp at the marked area.

6.5. Apply aortic clamping in ascending order of 1-, 2-, 5-, 10-, and 30-min intervals to improve the survival of the animals during the study protocol.

6.6. Continue aortic cross-clamping after each interval after a maximum of 5 min or after normalization of femoral artery flow.

6.7. Perform manual inflow occlusion of the inferior vena cava to prevent blood pressure increases of > 100 mmHg mean arterial pressure.

6.8. Administer bolus injections of norepinephrine or epinephrine during the clamping phase, if needed, to prevent decreases in mean arterial pressure below 40 mmHg.

6.9. Repeat measurements at the end of the 30-min clamping interval prior to reperfusion (M2).

6.10. Gradually open the clamp to ensure hemodynamic stability. Close the clamp if blood pressure drops too quickly and allow stabilization.

6.11. Administer 7 $mL \cdot kg^{-1}$ of hydroxyethyl starch colloids as well as additional bolus injections of 10–20 µg of norepinephrine and/or epinephrine for stabilization. Administer 2 $mL\ kg^{-1}$ of 8.4% sodium bicarbonate if the pH drops below 7.1. Ensure proper adjustment of the respiratory rate to ensure normocapnia.

6.12. Repeat measurements 1 h after reperfusion (M3).

6.13. Repeat hemodynamic optimization as described under 6.2, and repeat measurements (M4).

6.14. Perform final measurements 4.5 h after the induction of ischemia/reperfusion (M5).

7. Euthanasia

7.1. Administer 40 mmol of potassium chloride intravenously for euthanasia to induce ventricular fibrillation and asystole.

7.2. Terminate ventilation and remove all catheters.

8. Organ harvesting

8.1. Place the animal in a prone position, and remove the needle probes as well as the drainage.

8.2. Expose the spine by skin incision and removal of muscle tissue using a scalpel and forceps.

8.3. Use an oscillating saw to divide the vertebral arch paramedian on both sides, and remove the dorsal part of the vertebral bone by carefully moving the spinous process sideways to loosen the remaining connections.

8.4. Use forceps to carefully lift the spinal cord from the caudal to cranial ends, and use a scalpel to cut the spinal nerves to remove the spinal cord.

8.5. Store the spinal cord in 4% formalin until further utilization for histopathological evaluation or microsphere quantification.

9. Statistical analysis

9.1. Use statistical software.

9.2. Ensure normal distribution by inspection of histograms and log-transform variables if necessary.

9.3. Subject the dependent variables—spinal cord Flux, cardiac output, heart rate, stroke volume, systolic arterial pressure, mean arterial pressure, diastolic arterial pressure, central venous pressure, systemic vascular resistance, as well as upper and lower spinal cord microperfusion as assessed with fluorescent microspheres if desired—to general linear mixed model analyses, using the routine GENLINMIXED for continuous data with an identity link function.

9.4. Use baseline adjustments.

9.5. Specify models with fixed effects for variable baseline and measurement point. Consider measurement point as repeated measures within animals.

9.6. Report p-values of fixed effects for measurement point for each parameter.

9.7. For spinal cord fluorescent microsphere analysis, use region (lower spinal cord, upper spinal cord) in addition as fixed effect and interaction between region and measurement point to evaluate interactions between regions and measurement point, and report p-values of fixed effects for interaction as well.

9.8. Compute baseline adjusted marginal means with 95% confidence interval (CI) for all dependent variables at measurement points M1–M5, followed by pairwise comparisons via least significant difference tests.

9.9. Express variables as mean (95% CI). Express animal weight as mean ± standard deviation.

9.10. Present unadjusted p-values.

REPRESENTATIVE RESULTS:

All six animals survived until the completion of the protocol. Animal weight was 48.2 ± 2.9 kg; five animals were male, and one animal was female. Spinal cord needle probe insertion as well as spinal cord Flux measurement was feasible in all animals.

Examples of real-time spinal cord microcirculatory recordings in combination with cerebral microcirculatory and macrohemodynamic recordings during aortic cross-clamping for ischemia induction as well as during unclamping and reperfusion are shown in **Figure 3A,B**. The disruption of descending aortic flow was followed by a marked decrease in spinal cord Flux, while pressure in the ascending aortic increased (**Figure 3A**). Reperfusion led to opposite effects (**Figure 3B**).

Statistical analysis of macro- and microcirculatory parameters is shown in **Table 1**. Mixed-model-estimated marginal means and their confidence intervals indicate marked reduction of spinal cord Flux during ischemia. In contrast, cerebral Flux markedly increased during ischemia, as indicated by the estimated marginal means and their confidence intervals. This was accompanied by increase in arterial pressure, heart rate, and systemic vascular resistance, whereas cardiac output and stroke volume decreased. Fluorescent microsphere analysis revealed a marked decrease in spinal cord microcirculatory blood flow in the lower spinal cord, while there was no significant change in the upper spinal cord, as indicated by the estimated marginal means and their confidence intervals. Reperfusion led to opposite effects. Although there was a further decrease in cardiac output, stroke volume, and arterial pressure at the end of the protocol, spinal cord Flux as well as spinal cord microcirculatory blood flow were stable.

The results of this study show the ability of Laser/Doppler needle probes to detect real-time changes in spinal cord microperfusion. As expected, the decrease in spinal cord microcirculation during ischemia was drastic with minimal microcirculatory Flux. Recovery of spinal cord Flux occurred after reperfusion. Lower spinal cord perfusion, as assessed with fluorescent microspheres, showed a comparable behavior, thus supporting the method. As expected, upper spinal cord perfusion and cerebral Flux showed different behaviors. Although spinal cord microcirculation was stable, macrocirculation declined at the end of the protocol, showing a loss of hemodynamic coherence. While flow in the descending aorta was zero during ischemia, reperfusion led to a recovery of aortic flow. Histopathological analysis revealed mild necrosis of the spinal cord with Kleinman-scores for the lower spinal cord between 0 and 2 and for the upper spinal cord between 0 and 1.

FIGURE AND TABLE LEGENDS:

Figure 1: Placement of laser/Doppler needle probe in the spinal cord. (**A**) Surgical exposure of vertebral structures. (**B**) Puncture of the spinal cord using a vein catheter. (**C**) Insertion of the needle probe after removal of the inlay needle. (**D**) Fixation of the needle probe.

Figure 2: **Exposure of the descending aorta and placement of flow probe and vessel loop.** (**A**) Exposure of the descending aorta after mobilizing the apex of the left lung and dividing of the left-lateral part of the diaphragm. (**B**) Dividing of the surrounding tissue for surgical exposure. (**C**) Placement of an overhold around the descending aorta to secure proper circular exposure. (**D**) Placement of flow probe as well as vessel loop around the descending aorta.

Figure 3: Sample recordings of microcirculatory and macrohemodynamic signals during ischemia as well as reperfusion. Sample recordings of ECG, pressure in the ascending aorta as measured using a microtip-catheter, flow in the descending aorta as measured using an ultrasonic flow probe, spinal cord as well as cerebral microcirculatory FLUX as measured using laser/Doppler needle probes. (**A**) 50 s sample during ischemia induction by supra-celiac aortic cross-clamping. (**B**) 20 s sample during reperfusion induction by gentle re-opening of the aortic cross-clamp.

Table 1: Changes in hemodynamic parameters during the protocol. Values are given as baseline-adjusted estimated marginal means with 95% confidence intervals. Unadjusted p-values of F-tests of main effects of measurement point are given for each parameter as well as of interaction effects between region and measurement point for upper and lower spinal cord microperfusion. Unadjusted p-values of pairwise comparisons of individual measuring points with M1 are also presented. Measurement points are: M1 = Hemodynamic optimization prior ischemia/reperfusion, M2 = During ischemia, M3 = 1 h after reperfusion M4 = Hemodynamic optimization after ischemia/reperfusion, M5 = 4.5 h after induction of ischemia/reperfusion.

DISCUSSION:

SCI induced by spinal cord ischemia is a major complication of aortic repair with tremendous impact on patient outcome[1-4,10-12]. Microcirculation-targeted therapies to prevent and treat SCI are most promising. The protocol provides a reproducible method for real-time spinal cord microcirculatory evaluation and offers the ability to evaluate effects of novel therapeutic approaches on spinal cord microcirculation under ischemia/reperfusion conditions.

There are some critical methodological steps in this experimental model. To prevent loss of animals, researchers must be experienced in anesthesiologic techniques (cerebrospinal fluid drainage insertion, sonographic vascular access and hemodynamic therapy during aortic exposure, aortic cross-clamping, and reperfusion) as well as in surgical techniques (sternotomy, vessel exposure, surgical exposure of the descending aorta). Insertion of the spinal cord needle probe requires experience, profound knowledge of the anatomy, and sound technical skills. However, in our experience, the learning curve is considerably steep, and most experienced researchers will achieve success in a short time, although multiple attempts must be avoided to prevent spinal cord injuries that could affect the methodology.

Another critical step is the change from the right lateral to supine position to prevent dislocation or damage of the spinal cord needle probe. For this maneuver, 4–5 persons are recommended, proper padding of the insertion site is essential, and meticulous caution should be taken not to dislocate the probe. Exposure of the descending aorta requires some critical steps as well. The apex of the left lung must be mobilized to allow gentle retraction of the left lung to expose the surgical field. In addition, the left-lateral part of the diaphragm should be dissected to facilitate exposure. During aortic preparation, optimal communication between those researchers performing surgery and those providing anesthesia and hemodynamic management is needed to ensure adequate cardiopulmonary stability. During aortic cross-clamping, manual compression of the inferior vena cava is recommended to reduce venous return. Without this maneuver, severe afterload increases may occur that

could lead to deleterious myocardial injury[37,38].

Reperfusion should be performed cautiously with fluids, vasopressors, and inotropes ready to use. During reperfusion, dramatic changes occur that may lead to severe hypotension, cardiac arrythmias, and circulatory failure[39]. However, cautious observation of hemodynamic behavior, prompt initiation of interventions, as well as use of a structured and gentle performance during this critical phase can prevent loss of animals. In addition, the use of ascending intervals of aortic cross-clamping, followed by time periods to improve regeneration, as used in the protocol, induces ischemic pre-conditioning effects that enhance hemodynamic stability during reperfusion[40,41].

The model provides the ability to monitor spinal cord microcirculation in addition to macrocirculatory evaluation. Owing to the loss of hemodynamic coherence frequently seen in high-risk surgery and critically ill patients, direct evaluation of spinal cord microcirculation is necessary[13,28]. Sublingual microcirculation is often used to replace direct microcirculatory evaluation in the organ of interest[42]. However, dissociation between sublingual microcirculation and vital organs has been shown, emphasizing the value of direct microcirculatory evaluation in the spinal cord, as used in the experimental model[43]. Finally, the model has the advantage of real-time monitoring of spinal cord blood flow in comparison to fluorescent microsphere evaluation, which is limited by intermittent use and post-mortem analysis[44]. The impact of real-time assessment can best be seen when looking at example recordings during ischemia as well as reperfusion induction, showing rapid changes in spinal cord microperfusion. However, it should be considered that laser-Doppler probe insertion in the spinal cord could lead to small, but considerable, injuries of the spinal cord.

As the integrity of the spinal cord could possibly influence the hemodynamic parameters, this could be a disadvantage of the method. However, the use of laser-Doppler techniques to assess spinal cord microperfusion have been previously used[45-48]. Moreover, although we did not observe hemodynamic changes following probe insertion, we could not rule out hemodynamic effects induced by this method. It should be noted that hemodynamic alterations may also be induced by use of microsphere injections, which would, however, be of minor importance in large animals[49]. Moreover, sensory or motor function may be affected by probe insertion and therefore, use of sensory- or motor-evoked potential assessment should be performed with caution in combination with laser-Doppler evaluation.

In this regard, the microsphere injection technique might be advantageous. In addition, the techniques should not be used for chronic trials; however, this is also true for microsphere injections, which are limited to acute trials because they are dependent on post-mortem tissue analysis. Most studies using laser-Doppler techniques were performed in small animals[45-48]. Here, we describe a technique for use in pigs, as a large animal model, which could facilitate translation to clinical studies. The paramedian-introducing technique overcomes the problem of large spinous processes in pigs, which complicates proper placement of spinal cord probes. Moreover, the technique has the advantage that laminectomy or removal of dura tissue is not needed, preventing a constant loss of liquor. As the cerebrospinal fluid pressure has a tremendous impact on spinal cord perfusion[30], the model has the advantage of measuring and optimizing cerebrospinal fluid pressure in addition to spinal cord microperfusion and will address the effect of cerebrospinal fluid pressure on

spinal cord microperfusion in future projects.

The protocol has some limitations that should be mentioned. Absolute values of spinal cord Flux differ considerably between animals due to differences in exact probe position and proximity of larger spinal cord vessels. Therefore, baseline adjustments should be performed when comparing values. However, intra-individual differences between measurement points are highly consistent as long as meticulous caution is exercised to avoid movements of the needle probe during the protocol. Moreover, this study was not designed as a comparison study between the Laser-Doppler and the fluorescent microsphere methods. Given the number of animals, we did not perform a correlation analysis between these two methods.

Although both methods showed a comparable behavior with significant reductions during ischemia and recovery after reperfusion for both, a comparison of the methods should be addressed using properly designed studies in the future. Nevertheless, the use of microspheres additionally enabled evaluation of different behaviors for upper and lower spinal cord microperfusion. In addition, histopathological analysis revealed only moderate spinal cord necrosis compared to other models of spinal cord ischemia[35]. Prolonging the duration of ischemia as well as omitting pre-conditioning measures may lead to more severe changes that may be desired by some researchers. Although we evaluated only mild histopathological changes, this may be different with a longer duration of ischemia. In this regard, a longer period after ischemia/reperfusion prior to termination of the protocol may have also led to more severe histopathological changes. However, the protocol enabled hemodynamic stability one hour after reperfusion without the need for additional or even continuous inotrope or vasopressor application.

For the evaluation of different hemodynamic interventions, this model provides optimal conditions. Although we used fluid optimization as an example of hemodynamic intervention, other approaches may be evaluated with this method. While this protocol provides microcirculatory evaluation in a model of ischemia/reperfusion, the duration of ischemia limits the evaluation of therapeutic approaches during ischemia prior to reperfusion. Moreover, during ischemia, a variation in hemodynamic changes occurred (e.g., hypertension, hypotension, tachycardia, bradycardia, as well as cardiac arrythmias). Manual inflow occlusion further affects hemodynamic variables during this phase. Therefore, the protocol is not recommended for the evaluation of therapeutic approaches during ischemia prior to reperfusion. However, other experimental settings, such as the use of embolization or ligation techniques, may be combined with spinal cord laser/Doppler needle probe evaluation, as described in this protocol.

ACKNOWLEDGMENTS:
The authors would like to thank Lena Brix, V.M.D, Institute of Animal Research, Hannover Medical School, as well as Mrs. Jutta Dammann, Facility of Research Animal Care, University Medical Center Hamburg-Eppendorf, Germany, for providing pre- and perioperative animal care and their technical assistance on animal handling. The authors would further like to thank Dr. Daniel Manzoni, Department of Vascular Surgery, Hôpital Kirchberg, Luxembourg, for his technical assistance.

DISCLOSURES:

Constantin J. C. Trepte has received an honorary award for lectures by Maquet. All other authors declare no conflicts of interest. This study was supported by the European Society of Anaesthesiology Young Investigator Start-Up Grant 2018.

REFERENCES:

1 Etz, C. D. et al. Contemporary spinal cord protection during thoracic and thoracoabdominal aortic surgery and endovascular aortic repair: a position paper of the vascular domain of the European Association for Cardio-Thoracic Surgerydagger. *The European Journal of Cardio-Thoracic Surgery.* **47** (6), 943-957 (2015).

2 Schraag, S. Postoperative management. *Best Practice & Research Clinical Anaesthesiology.* **30** (3), 381-393 (2016).

3 Cambria, R. P. et al. Thoracoabdominal aneurysm repair: results with 337 operations performed over a 15-year interval. *Annals of Surgery.* **236** (4), 471-479; discussion 479 (2002).

4 Becker, D. A., McGarvey, M. L., Rojvirat, C., Bavaria, J. E., Messe, S. R. Predictors of outcome in patients with spinal cord ischemia after open aortic repair. *Neurocritical Care.* **18** (1), 70-74 (2013).

5 McGarvey, M. L. et al. The treatment of spinal cord ischemia following thoracic endovascular aortic repair. *Neurocritical Care.* **6** (1), 35-39 (2007).

6 Fukui, S. et al. Development of collaterals to the spinal cord after endovascular stent graft repair of thoracic aneurysms. *European Journal of Vascular and Endovascular Surgery.* **52** (6), 801-807 (2016).

7 Augoustides, J. G., Stone, M. E., Drenger, B. Novel approaches to spinal cord protection during thoracoabdominal aortic interventions. *Current Opinion in Anesthesiology.* **27** (1), 98-105 (2014).

8 Bicknell, C. D., Riga, C. V., Wolfe, J. H. Prevention of paraplegia during thoracoabdominal aortic aneurysm repair. *European Journal of Vascular and Endovascular Surgery.* **37** (6), 654-660 (2009).

9 Feezor, R. J., Lee, W. A. Strategies for detection and prevention of spinal cord ischemia during TEVAR. *Seminars in Vascular Surgery.* **22** (3), 187-192 (2009).

10 Heidemann, F. et al. Incidence, predictors, and outcomes of spinal cord ischemia in elective complex endovascular aortic repair: An analysis of health insurance claims. *Journal of Vascular Surgery.* doi:10.1016/j.jvs.2019.10.095, (2020).

11 Rizvi, A. Z., Sullivan, T. M. Incidence, prevention, and management in spinal cord protection during TEVAR. *Journal of Vascular Surgery.* **52** (4 Suppl), 86S-90S (2010).

12 Wortmann, M., Bockler, D., Geisbusch, P. Perioperative cerebrospinal fluid drainage for the prevention of spinal ischemia after endovascular aortic repair. *Gefasschirurgie.* **22** (Suppl 2), 35-40 (2017).

13 Saugel, B., Trepte, C. J., Heckel, K., Wagner, J. Y., Reuter, D. A. Hemodynamic management of septic shock: is it time for "individualized goal-directed hemodynamic therapy" and for specifically targeting the microcirculation? *Shock.* **43** (6), 522-529 (2015).

14 Moore, J. P., Dyson, A., Singer, M., Fraser, J. Microcirculatory dysfunction and resuscitation: why, when, and how. *British Journal of Anaesthesia.* **115** (3), 366-375 (2015).

15 De Backer, D., Creteur, J., Preiser, J. C., Dubois, M. J., Vincent, J. L. Microvascular blood flow is altered in patients with sepsis. *American Journal of Respiratory and Critical Care Medicine.* **166** (1), 98-104 (2002).

16 De Backer, D., Creteur, J., Dubois, M. J., Sakr, Y., Vincent, J. L. Microvascular alterations in patients with acute severe heart failure and cardiogenic shock. *American Heart Journal.* **147**

(1), 91-99 (2004).
17 Sakr, Y., Dubois, M. J., De Backer, D., Creteur, J., Vincent, J. L. Persistent microcirculatory alterations are associated with organ failure and death in patients with septic shock. *Critical Care Medicine.* **32** (9), 1825-1831 (2004).
18 Trzeciak, S. et al. Early microcirculatory perfusion derangements in patients with severe sepsis and septic shock: relationship to hemodynamics, oxygen transport, and survival. *Annals of Emergency Medicine.* **49** (1), 88-98, 98 e81-82 (2007).
19 Donati, A. et al. From macrohemodynamic to the microcirculation. *Critical Care Research and Practice.* **2013** 892710 (2013).
20 Hamamoto, Y., Ogata, T., Morino, T., Hino, M., Yamamoto, H. Real-time direct measurement of spinal cord blood flow at the site of compression: relationship between blood flow recovery and motor deficiency in spinal cord injury. *Spine (Phila Pa 1976).* **32** (18), 1955-1962 (2007).
21 Soubeyrand, M. et al. Real-time and spatial quantification using contrast-enhanced ultrasonography of spinal cord perfusion during experimental spinal cord injury. *Spine (Phila Pa 1976).* **37** (22), E1376-1382 (2012).
22 Han, S*. et al.* Rescuing vasculature with intravenous angiopoietin-1 and alpha v beta 3 integrin peptide is protective after spinal cord injury. *Brain.* **133** (Pt 4), 1026-1042 (2010).
23 Muradov, J. M., Ewan, E. E., Hagg, T. Dorsal column sensory axons degenerate due to impaired microvascular perfusion after spinal cord injury in rats. *Experimental Neurology.* **249**, 59-73 (2013).
24 Ospina-Tascon, G. et al. Effects of fluids on microvascular perfusion in patients with severe sepsis. *Intensive Care Medicine.* **36** (6), 949-955 (2010).
25 Pottecher, J. et al. Both passive leg raising and intravascular volume expansion improve sublingual microcirculatory perfusion in severe sepsis and septic shock patients. *Intensive Care Medicine.* **36** (11), 1867-1874 (2010).
26 De Backer, D., Ortiz, J. A., Salgado, D. Coupling microcirculation to systemic hemodynamics. *Current Opinion in Critical Care.* **16** (3), 250-254 (2010).
27 van Genderen, M. E. et al. Microvascular perfusion as a target for fluid resuscitation in experimental circulatory shock. *Critical care medicine.* **42** (2), e96-e105 (2014).
28 Ince, C. Hemodynamic coherence and the rationale for monitoring the microcirculation. *Critical care.* **19 Suppl 3** S8 (2015).
29 Kise, Y. et al. Directly measuring spinal cord blood flow and spinal cord perfusion pressure via the collateral network: correlations with changes in systemic blood pressure. *Journal of Thoracic and Cardiovascular Surgery.* **149** (1), 360-366 (2015).
30 Haunschild, J. et al. Detrimental effects of cerebrospinal fluid pressure elevation on spinal cord perfusion: first-time direct detection in a large animal model. *European Journal of Cardio-Thoracic Surgery.* **58** (2), 286-293 (2020).
31 Wipper, S. et al. Impact of hybrid thoracoabdominal aortic repair on visceral and spinal cord perfusion: The new and improved SPIDER-graft. *Journal of Thoracic and Cardiovascular Surgery.* **158** (3), 692-701 (2019).
32 Kluttig, R. et al. Invasive hemodynamic monitoring of aortic and pulmonary artery hemodynamics in a large animal model of ARDS. *Journal of Visualized Experiments.* (141), doi:10.3791/57405, (2018).
33 Detter, C. et al. Fluorescent cardiac imaging: a novel intraoperative method for quantitative assessment of myocardial perfusion during graded coronary artery stenosis. *Circulation.* **116** (9), 1007-1014 (2007).

34 Wipper, S. et al. Distinction of non-ischemia inducing versus ischemia inducing coronary stenosis by fluorescent cardiac imaging. *International Journal of Cardiovascular Imaging.* **32** (2), 363-371 (2016).
35 Etz, C. D. et al. Spinal cord blood flow and ischemic injury after experimental sacrifice of thoracic and abdominal segmental arteries. *European Journal of Cardio-Thoracic Surgery.* **33** (6), 1030-1038 (2008).
36 Saugel, B., Scheeren, T. W. L., Teboul, J. L. Ultrasound-guided central venous catheter placement: a structured review and recommendations for clinical practice. *Critical care.* **21** (1), 225 (2017).
37 Marty, B. et al. Partial inflow occlusion facilitates accurate deployment of thoracic aortic endografts. *Journal of Endovascular Therapy.* **11** (2), 175-179 (2004).
38 Matyal, R. et al. Monitoring the variation in myocardial function with the Doppler-derived myocardial performance index during aortic cross-clamping. *Journal of Cardiothoracic and Vascular Anesthesia.* **26** (2), 204-208 (2012).
39 Miller, R. D. *Miller's anesthesia*. 8th Edition, (Philadelphia: Elsevier, 2015).
40 Martikos, G. et al. Remote ischemic preconditioning decreases the magnitude of hepatic ischemia-reperfusion injury on a swine model of supraceliac aortic cross-clamping. *Annals of Vascular Surgery.* **48**, 241-250 (2018).
41 Lazaris, A. M. et al. Protective effect of remote ischemic preconditioning in renal ischemia/reperfusion injury, in a model of thoracoabdominal aorta approach. *Journal of Surgical Research.* **154** (2), 267-273 (2009).
42 Ince, C. et al. Second consensus on the assessment of sublingual microcirculation in critically ill patients: results from a task force of the European Society of Intensive Care Medicine. *Intensive Care Medicine.* **44** (3), 281-299 (2018).
43 Edul, V. S. et al. Dissociation between sublingual and gut microcirculation in the response to a fluid challenge in postoperative patients with abdominal sepsis. *Annals of intensive care.* **4,** 39, doi:10.1186/s13613-014-0039-3, (2014).
44 Schierling, W. et al. Sonographic real-time imaging of tissue perfusion in a porcine haemorrhagic shock model. *Ultrasound in Medicine and Biology.* **45** (10), 2797-2804 (2019).
45 Jing, Y., Bai, F., Chen, H., Dong, H. Using Laser Doppler Imaging and Monitoring to Analyze Spinal Cord Microcirculation in Rat. *Journal of Visualized Experiments.* (135), doi:10.3791/56243, (2018).
46 Jing, Y., Bai, F., Chen, H., Dong, H. Meliorating microcirculatory with melatonin in rat model of spinal cord injury using laser Doppler flowmetry. *Neuroreport.* **27** (17), 1248-1255 (2016).
47 Jing, Y., Bai, F., Chen, H., Dong, H. Melatonin prevents blood vessel loss and neurological impairment induced by spinal cord injury in rats. *Journal of Spinal Cord Medicine.* **40** (2), 222-229 (2017).
48 Phillips, J. P., Cibert-Goton, V., Langford, R. M., Shortland, P. J. Perfusion assessment in rat spinal cord tissue using photoplethysmography and laser Doppler flux measurements. *Journal of Biomedical Optics.* **18** (3), 037005 (2013).
49 Glenny, R. W., Bernard, S. L., Lamm, W. J. Hemodynamic effects of 15-microm-diameter microspheres on the rat pulmonary circulation. *Journal of Applied Physiology (1985).* **89** (2), 499-504 (2000).

Fig. 1

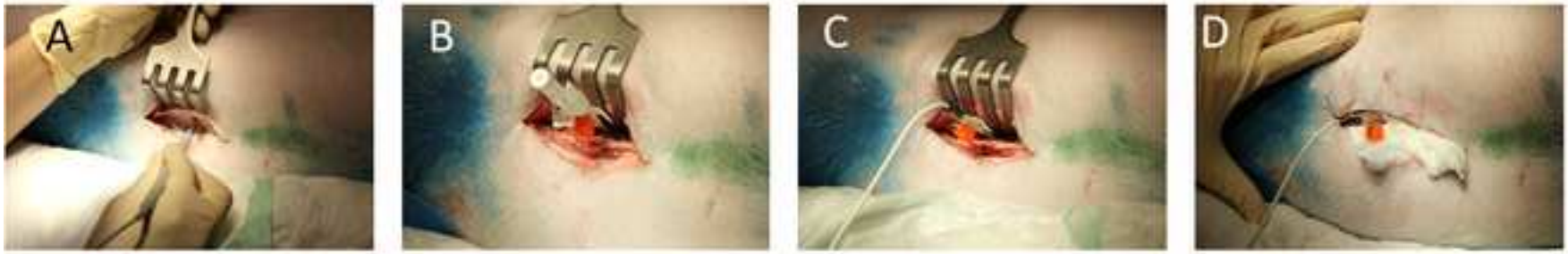

Figure 2

Click here to access/download;Figure;Folie2.TIF

Fig. 2

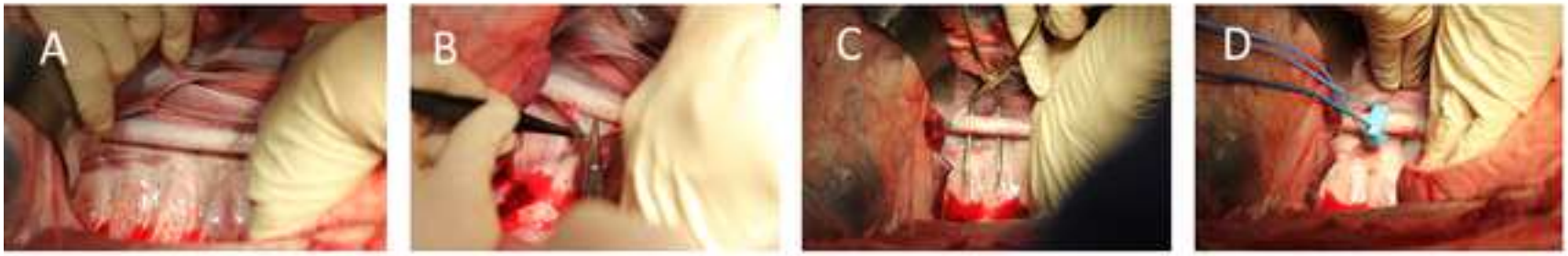

Figure 3 a

Click here to access/download;Figure;Folie3.TIF

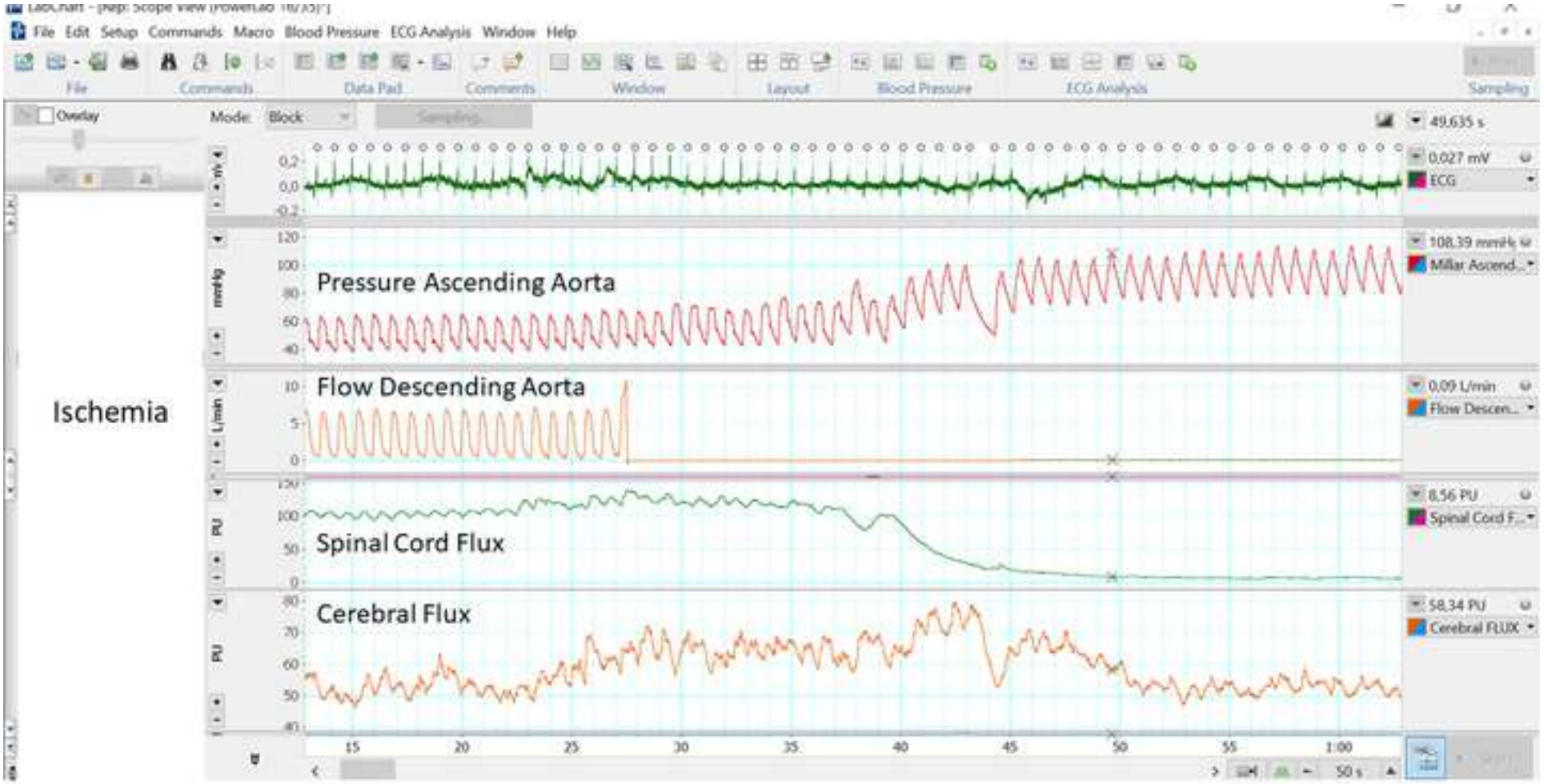

Fig. 3 A

Figure 3 b

Click here to access/download;Figure;Folie4.TIF

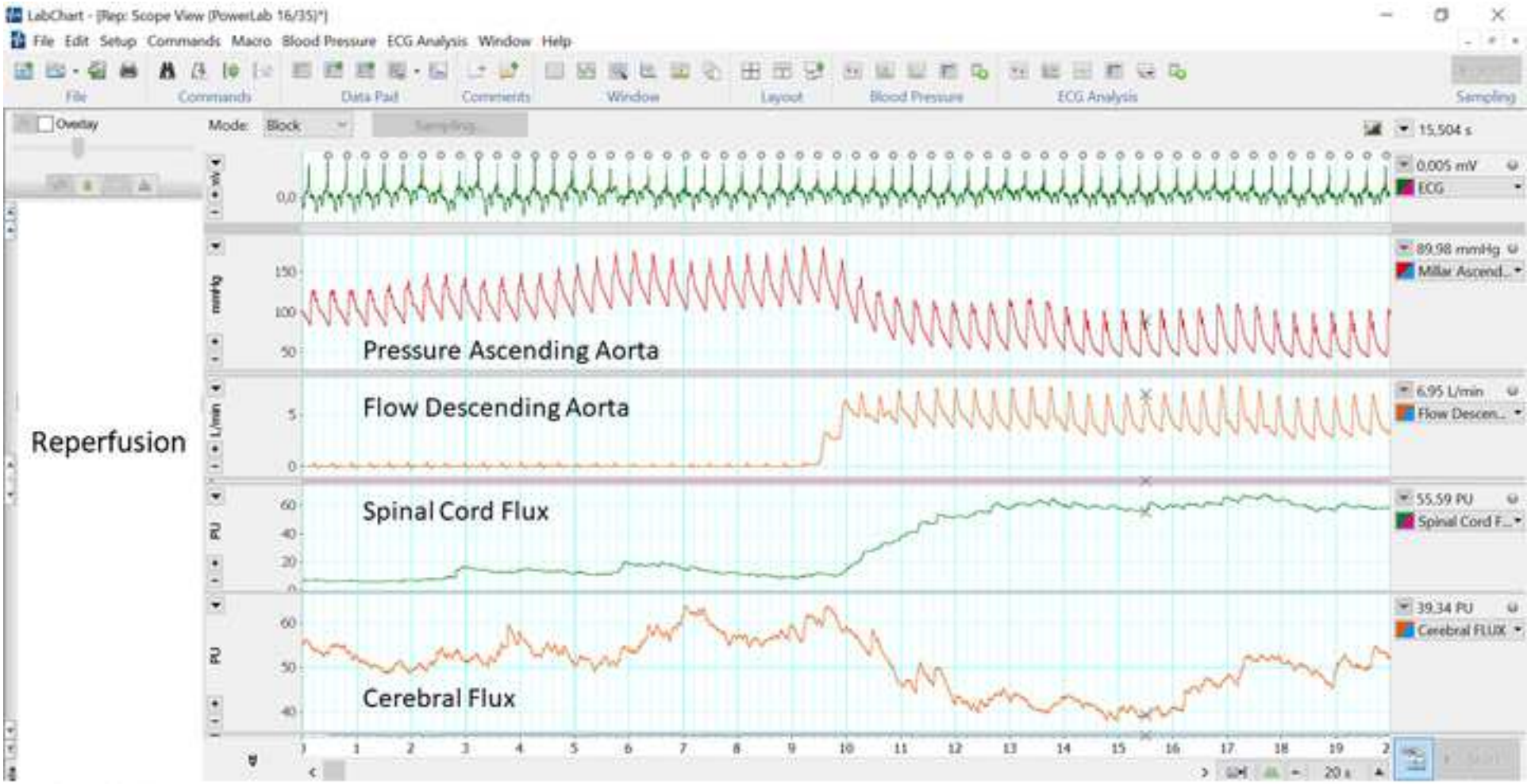

Fig. 3 B

Table

Table 1: Changes of hemodynamic parameters during the protocol		M1
Spinal Cord Flux main effect measurement point: p < 0.001		61.35 (41.96-89.70)
Cerebral Flux main effect measurement point: p = 0.023		41.12 (28.17-60.04)
Spinal Cord Microperfusion (mL/min/g) main effect measurement point: p < 0.001 interaction measurement point x spinal cord location: p < 0.001	Lower spinal cord	0.071 (0.058-0.087)
	Upper spinal cord	0.079 (0.065-0.097)
Cardiac Output (L/min) main effect measurement point: p < 0.001		4.15 (3.69-4.61)
Heart Rate (bpm) main effect measurement point: p = 0.002		74.42 (53.70-95.15)
Stroke Volume (mL) main effect measurement point: p < 0.001		55.50 (49.20-61.81)
Systolic Arterial Pressure (mmHg) Ascending Aorta main effect measurement point: p < 0.001		94.36 (85.20-103.52)
Mean Arterial Pressure (mmHg) Ascending Aorta main effect measurement point: p < 0.001		78.18 (68.68-87.67)
Diastolic Arterial Pressure (mmHg) Ascending Aorta main effect measurement point: p < 0.001		59.20 (49.41-69.00)
Systemic Vascular Resistance (dyn/sec/cm^{-5}) main effect measurement point: p < 0.001		1421.13 (1236.94-1632.74)
Flow (L/min) Descending Aorta main effect measurement point: p = 0.003		3.27 (0.96-5.58)

M2	M3	M4	M5
6.78 (4.63-9.91) p < 0.001	58.97 (40.33-86.22) p = 0.878	66.05 (45.17-96.57) p = 0.777	59.09 (40.41-86.40) p = 0.886
71.73 (49.13-104.73) p = 0.001	60.34 (41.33-88.10) p = 0.045	59.91 (36-93-78.71) p = 0.173	49.82 (34.12-72.74) p = 0.341
0.063 (0.052-0.078) p = 0.420	0.088 (0.072-0.11) p = 0.146	0.082 (0.067-0.100) p = 0.344	0.083 (0.068-0.102) p = 0.281
0.031 (0.026-0.039) p < 0.001	0.111 (0.090-0.136) p = 0.021	0.089 (0.073-0.110) p = 0.400	0.105 (0.086-0.129) p = 0.051
3.13 (2.67-3.60) p < 0.001	3.30 (2.84-3.76) p = 0.007	3.67 (3.20-4.13) p = 0.125	2.67 (2.00-2.93) p < 0.001
131.09 (110.36-151.82) p < 0.001	88.92 (68.19-109.65) p = 0.314	80.62 (59.89-101.35) p = 0.666	99.38 (78.65-120.11) p = 0.092
25.33 (19.03-31.64) p < 0.001	37.00 (30.69-43.31) p < 0.001	45.33 (39.03-51.64) p = 0.004	27.17 (20.86-33.47) p < 0.001
122.05 (112.89-131.20) p < 0.001	76.72 (67.56-85.88) p = 0.006	88.36 (79.20-97.52) p = 0.321	73.36 (64.20-82.52) p = 0.002
107.29 (97.80-116.78) p < 0.001	59.08 (49.58-68.57) p = 0.005	70.38 (60.89-79.87) p = 0.217	58.35 (48.85-67.84) p = 0.004
93.76 (83.97-103.56) p < 0.001	45.18 (35.38-54.98) p = 0.038	52.48 (42.69-62.28) p = 0.302	45.33 (35.54-55.13) p = 0.040
208089.94 (181128.10-239085.87) p < 0.001	1335.36 (1162.29-1534.21) p = 0.407	1412.62 (1229.54-1622.97) p = 0.938	1807.46 (1573.21-2076.60) p = 0.005
0	3.27 (0.96-5.58) p = 0.998	3.54 (1.23-5.85) p = 0.844	4.54 (2.32-6.85) p = 0.381

Table of Materials

Name of Material/ Equipment	**Company**
CardioMed Flowmeter	Medistim AS, Oslo, Norway
CardioMed Flow-Probe, 5mm	Medistim AS, Oslo, Norway
COnfidence probe, 16 mm liners	Transonic Systems Inc., Ithaca, NY, USA
DIVA Sevoflurane Vapor	Dräger Medical, Lübeck, Germany
Hotline Level 1 Fluid Warmer	Smiths Medical Germany GmbH, Grasbrunn, Germany
Infinity Delta	Dräger Medical, Lübeck, Germany
Infinity Hemo	Dräger Medical, Lübeck, Germany
LabChart Pro	ADInstruments Ltd., Oxford, UK
LiquoGuard 7	Möller Medical GmbH, Fulda, Germany
Millar Micro-Tip Pressure Catheter (5F, Single, Curved, 120cm, PU/WD)	ADInstruments Ltd., Oxford, UK
moor VMS LDF	moor Instruments, Devon, UK
moor VMS Research Software	moor Instruments, Devon, UK
Perivascular Flow Module	Transonic Systems Inc., Ithaca, NY, USA
PiCCO 2, Science Version	Getinge AB, Göteborg, Sweden
PiCCO 5 Fr. 20cm	Getinge AB, Göteborg, Sweden
PowerLab	ADInstruments Ltd., Oxford, UK
QuadBridgeAmp	ADInstruments Ltd., Oxford, UK
Silverline	Spiegelberg, Hamburg, Germany
SPSS statistical software package	IBM SPSS Statistics Inc., Armonk, New York, USA
Twinwarm Warming System	Moeck & Moeck GmbH, Hamburg, Germany
Universal II Warming Blanket	Moeck & Moeck GmbH, Hamburg, Germany
VP 3 Probe, 8mm length (individually manufactured)	moor Instruments, Devon, UK
Zeus	Dräger Medical, Lübeck, Germany

Catalog Number	Comments/Description
CM4000	Flowmeter for Flow-Probe Femoral Artery
PS100051	Flow-Probe Femoral Artery
MA16PAU	Flow-Probe Aorta
	Vapor
HL-90-DE-230	Fluid Warmer
	Basic Monitoring Hardware
	Basic Pressure Monitoring and Pulmonary Thermodilution Hardware
v8.1.16	Synchronic Laser-Doppler, Blood Pressure, ECG and Blood-Flow Aquisition Software
	Cerebrospinal Fluid Drainage System
SPR-350	Pressure-Tip Catheter Aorta
	Designated Laser-Doppler Hardware
	Designated Laser-Doppler Software
TS 420	Flow-Module for Flow-Probe Aorta
v. 6.0	Blood Pressure and Transcardiopulmonary Monitoring Hard- and Software
	Thermistor-tipped Arterial Line
PL 3516	Synchronic Laser-Doppler, Blood Pressure, ECG and Blood-Flow Aquisition Hardware
FE 224	Four Channel Bridge Amplifier for Laser-Doppler and Invasive Blood Pressure Aquisition
ELD33.010.02	Cerebrospinal Fluid Drainage
v. 27	Statistical Software
12TW921DE	Warming System
906	Warming Blanket
	Laser-Doppler Probe
	Anesthesia Machine

Editorial comments:

Changes to be made by the Author(s):

1. Please take this opportunity to thoroughly proofread the manuscript to ensure that there are no spelling or grammar issues. Please define all abbreviations at first use.

We thank the editor for this suggestion. We have proofread the manuscript and corrected spelling and grammar issues. All abbreviations are now defined at first use.

2. For in-text formatting, corresponding reference numbers should appear as numbered superscripts after the appropriate statement(s), but before punctuation.

We thank the editor for this advice and have corrected the reference numbers.

3. Lines 100-101: What do you mean by “Most of existing studies have used microsphere injection techniques which are limited by intermittent use and post-mortem analysis”?

We apologize to the editor for this phrasing and have changed this section to be more clearly. Microsphere injection technique uses fluorescent microspheres with different wavelengths. The number of different measurements is limited by the existence of microspheres with different wavelengths. The microspheres we used are only available in seven different colors, therefore a maximum of seven different measurements is possible. Moreover, in contrary to Laser-Doppler technique, microspheres cannot be used to assess microperfusion in real-time, since post-mortem analysis of tissue is needed. In additions, since also a number of studies exist that use other techniques including Laser-Doppler technique to assess spinal cord microcirculation, we have changed the wording of this part.

4. Please include a one line space between each protocol step and then highlight up to 3 pages of protocol text for inclusion in the protocol section of the video. Currently, there is about 3 pages of protocol text highlighted but without the one line space.

We thank the reviewer for this comment. We have included a one line space between protocol steps and have limited the highlighted protocol to 3 pages using this formatting.

5. 1.4: What are the parameters at baseline for ECG and pulse oximetry?

We agree with the reviewer, that this part needs to be clarified. “Basic” instead of “baseline” ECG and pulse oximetry was meant and these parameters were used throughout the entire procedure to ensure cardio-pulmonary stability of animals but were used for monitoring purposes only and not analyzed further to be presented in the results section. ECG needle probes described under 5.2. were used in addition to record an electrocardiogram. However, for this study it was not further analyzed and heart rate was assessed by blood pressure analysis. We have changed the section 1.4 accordingly.

6. 1.4, 2.4: Which adapted hardware and software are you referring to?

We apologize, for being unclear. We have changed the description of materials in the table of materials and have changed the protocol now clearly describing each hardware and software properly. Please see table of material and section 1.4, 2.4, as well as 2.10, 2.12, 2.15, 3.5, 3.6, 3.10, 3.11, 3.12, 4.9., 5.2., 5.4..

7. 2.13: How do you calibrate flux as PU with 2-point calibration?

We agree with the editor, that this part has to be described more clearly and have described this under section 2.16.

8. a) Please specify the euthanasia method without highlighting it.

We have now divided this section in two parts, section 7 presents details on euthanasia. Part 8 describes organ harvesting and included the highlighted sections. Moreover, the method of euthanasia is now more clearly described.

b) Please mention how animals are anesthetized and how proper anesthetization is confirmed.

We apologize if there were any uncertainties. We have summarized the methods of anesthesia in section 1.1. Further details and anesthesia were already described in section 1.2, 1.11. Confirmation of proper anesthetization is also described in section 1.11. However, we have adapted section 1.2. as well as 1.11 to be more clearly.

c) Please specify the use of vet ointment on eyes to prevent dryness while under anesthesia.

We apologize for this omission. We did not use ointment on eyes, however we secured closure of eyes to prevent dryness of eyes. We have added this part under section 1.10.

d) For survival strategies, discuss post-surgical treatment of animal, including recovery conditions and treatment for post-surgical pain.

As this was an acute trial, we did not include details on post-surgical treatment since animals were euthanized during deep anesthesia at the end of the protocol. We have adapted the introduction to the protocol clearly stating that this was an acute trial.

e) Discuss maintenance of sterile conditions during survival surgery.

As this was an acute trial, we only applied semi-sterile conditions. We have included details on this issue as section 1.13.

f) Please specify that the animal is not left unattended until it has regained sufficient consciousness to maintain sternal recumbency.

As this was an acute trial, none of the animals regained consciousness. Instead, they were euthanatized in deep anesthesia. Researchers experienced with animal anesthesia were present during the entire procedure as described in part 1.11.

g) Please specify that the animal that has undergone surgery is not returned to the company of other animals until fully recovered.

Given that this was an acute trial, all animals were euthanized during deep anesthesia at the end of the protocol and cadavers were burnt after organ harvesting.

9. Please remove the embedded Tables from the manuscript. All tables should be uploaded separately to your Editorial Manager account in the form of an .xls or .xlsx file. Each table must be accompanied by a title and a description after the Representative Results of the manuscript text.

We thank the editor for this advice and have removed the tables and included them as separate tables.

10. Please ensure that the references appear as the following: [Lastname, F.I., LastName, F.I., LastName, F.I. Article Title. Source. Volume (Issue), FirstPage – LastPage (YEAR).] For more than 6 authors, list only the first author then et al. Please do not abbreviate journal names.

We thank the editor for this advice and have adapted the references accordingly.

Reviewers' comments:

Reviewer #1:

Manuscript Summary:

The author used laser-Doppler probe to measure changes in micro-circulation in spinal cord as a result of aortic sternotomy in pigs. The protocol is very well described.

We thank the reviewer for this compliment.

Major Concerns:

Authors mentioned that they compare the laser-Doppler data to that with fluorescent microsphere analysis but this correlation is hard to find.

We totally agree that this issue should be addressed more clearly. This study was not designed as a comparison study to compare Laser-Doppler-Method with fluorescent microspheres technique. The animal number was not sufficient to reliably compare these methods and we did not perform correlation analysis. Microsphere injection technique was used as additional technique as part of the large animal project and we presented the results in addition to provide information whether the different methods showed comparable behavior to additionally verify the Laser-Doppler method. Since both methods showed significant reductions during ischemia and recovery after reperfusion, we think that reporting microsphere analysis supports our method. In addition, microspheres were used to compare upper and lower spinal cord perfusion. However, we agree that correlation of these methods would be interesting and suggested that studies comparing both methods should be performed in the future. We included this limitation and have changed the abstract and the limitation section accordingly.

Minor Concerns:

There are previous publications that used laser-Doppler method to measure blood flow to spinal cord. Can authors articulate what is/are new features the method described?

We thank the reviewer for raising this question. We are glad to comment on this issue. Our method is different for three reasons:

1. Most of animal studies are performed in small animals (for example Jing et al. [1-3], Phillips et al.[4]). In rats and mice access of spinal cord may be easier. Here we describe a technique for use in pigs as a large animal model. Use of large animal models could facilitate translation to clinical studies and are therefore most interesting.
2. In pigs, the large spinous processes complicate proper placement of spinal cord probes. However, using a paramedian approach as described in our protocol overcomes this problem without need for removal of bone structures.
3. Our technique has the advantage, that laminectomy or removal of dura tissue is not needed that would lead to a constant loss of liquor. Since the cerebrospinal fluid pressure has a tremendous impact on spinal cord perfusion[5], our model has the advantage of measuring cerebrospinal fluid pressure in addition to spinal cord microperfusion and to address the effect of cerebrospinal fluid pressure on spinal cord microperfusion in future projects.

We have mentioned these differences to existing publications in the discussion as well.

Reviewer #2:

Manuscript Summary:

I would like to congratulate the authors for the present study. Well-designed and important preclinical work of interest to specialists in the field.

We thank the reviewer for this compliment.

Minor Concerns:

-Methods: please provide mean and standard deviation for the age of the animals. Further, indicate how the ratio between female/male pigs was? 1:1? This will help to maintain the reproducibility of the work.

We thank the reviewer for this suggestion and have added information on female male ratio in the results section. However, we have no information of the exact age of animals, as this was not provided by the breeder of animals. However, we have included mean and standard deviation of animals in the results section. Animals weighing between 42-51 kg of the used race (German landrace pig) would be 13-15 weeks old.

-Methods: It would be good to indicate whether microspheres injection was performed before or after hemodynamic optimization as the injection of the microspheres could potentially affect hemodynamics.

The reviewer raises an important issue and we are glad to comment on this issue. Microsphere injection for each measurement step was performed after recording of macro- and microcirculatory parameters. For measurement step M1 and M4, recording of macro- and microcirculatory parameters were performed after completion of hemodynamic optimization followed by microsphere injection. We have included information on this issue in and have adapted section 6.3. However, hemodynamic effects of microsphere in large animals as used in our study should be of minor importance[6].

-Discussion: as we have no sham-treated control group in this study design, it would have been interesting to discuss if laser-Doppler as the main methodological approach of this study would affect hemodynamics or has other known flaws. Pro/contra of this methodological approach compared to the mentioned microsphere technique has not been sufficiently discussed. This will help other researchers to choose between these two methodological techniques for their experiments.

The reviewer raises an important aspect. Since the laser-Doppler probe needs to be inserted in the spinal cord, this may lead to small but considerable injuries of the spinal cord. Since the integrity of spinal cord could possibly influence hemodynamic parameters, this could speak against our method. However, use of laser-Doppler techniques to assess spinal cord microperfusion have been used previously ([1-4]). In regard to hemodynamic effects, we did not observe hemodynamic changes following probe insertion, nonetheless we could not rule out hemodynamic effects induced by this method. We agree with the reviewer, that hemodynamic alterations also can be seen after microsphere injections, however, in large animals this would be of minor importance. In regard to hemodynamic effects, we believe that both methods are acceptable. Moreover, sensory or motor function may be affected by probe insertion and therefore combination of sensory or motor evoked potential assessment should be performed with caution in combination with laser-Doppler evaluation. In this regard, microspheres might be advantageous. In addition, our techniques should not be used for chronic trials, however, this is also true for microsphere injections, which are limited to acute trials as well due to the fact that they are dependent on post-mortem tissue analysis. We have included this information for pro/contra comparison between methods in addition to the already mentioned facts in the discussion (real-time vs. post mortem analysis, unlimited measurement steps vs. limited measurements due to existing microspheres with different wavelength).

Additional comment: Interestingly, you found histological changes after 4.5 hours of intervention. A similar study in the field (DOI: 10.1002/ca.23586) has indicated that they found no differences in histological outcomes after 3 hours of intervention compared to the untreated sham group. Do you think this timeframe is enough to evaluate histological changes sufficiently? If not, please mention this in your discussion section so that other researches can choose longer time frames for their experiments for histological outcome measurements.

We thank the reviewer for this comment. As we did not use a sham group, we could not rule out effects other than ischemia/reperfusion. We have included this limitation. We agree with the reviewer, that a longer timeframe could have revealed different histological effects. As mentioned, histological evaluation showed only mild changes and this may be different by use of a longer timeframe. In addition to the suggestion of choosing a longer ischemic period we have added this suggestion to the discussion.

1 Jing, Y., Bai, F., Chen, H. & Dong, H. Using Laser Doppler Imaging and Monitoring to Analyze Spinal Cord Microcirculation in Rat. *J Vis Exp.* (135), doi:10.3791/56243, (2018).

2 Jing, Y., Bai, F., Chen, H. & Dong, H. Meliorating microcirculatory with melatonin in rat model of spinal cord injury using laser Doppler flowmetry. *Neuroreport.* **27** (17), 1248-1255, doi:10.1097/WNR.0000000000000686, (2016).

3 Jing, Y., Bai, F., Chen, H. & Dong, H. Melatonin prevents blood vessel loss and neurological impairment induced by spinal cord injury in rats. *J Spinal Cord Med.* **40** (2), 222-229, doi:10.1080/10790268.2016.1227912, (2017).

4 Phillips, J. P., Cibert-Goton, V., Langford, R. M. & Shortland, P. J. Perfusion assessment in rat spinal cord tissue using photoplethysmography and laser Doppler flux measurements. *J Biomed Opt.* **18** (3), 037005, doi:10.1117/1.JBO.18.3.037005, (2013).

5 Haunschild, J. *et al.* Detrimental effects of cerebrospinal fluid pressure elevation on spinal cord perfusion: first-time direct detection in a large animal model. *Eur J Cardiothorac Surg.* **58** (2), 286-293, doi:10.1093/ejcts/ezaa038, (2020).

6 Glenny, R. W., Bernard, S. L. & Lamm, W. J. Hemodynamic effects of 15-microm-diameter microspheres on the rat pulmonary circulation. *J Appl Physiol (1985).* **89** (2), 499-504, doi:10.1152/jappl.2000.89.2.499, (2000).